The Pennsylvania State University

The Graduate School

Department of Civil and Environmental Engineering

RETROFIT OPTIMIZATION FOR RESILIENCE ENHANCEMENT OF BRIDGES MULTIHAZARD SCENARIO

A Thesis in

Civil Engineering

by

Sandhya Chandrasekaran

Submitted in Partial Fulfillment
of the Requirements
for the Degree of

Master of Science

August 2014

The thesis of Sandhya Chandrasekaran was reviewed and approved* by the following:

Swagata Banerjee Basu
Assistant Professor of Civil Engineering
Thesis Advisor

Maria Lopez de Murphy
Associate Professor of Civil Engineering

Presanjit Basu
Assistant Professor of Civil Engineering

Prof. Peggy Johnson
Professor
Head of the Department of Civil Engineering

*Signatures are on file in the Graduate School

ABSTRACT

Bridge performance is often controlled by the strength of its critical sub-structural components (Teng *et. al* 2000). The seismic response of highway bridges is governed significantly by the axial strength and ductility of its columns. Prior to 1971, bridge failures were often characterized by column failures at the plastic hinge zones due to poor detailing and insufficient confinement (Ramanathan 2012). The Caltrans Seismic Retrofit Program adopted the technique of column jacketing to provide the additional confinement required to restrict the lateral disintegration of column concrete. Steel jackets have been established as a means to increase the deformation capacity of concrete beyond its unconfined compressive strength and consequently improve the column rotational ductility under lateral loading. However, fiber reinforced polymer (FRP) is growing as a preferred alternative owing to its high strength to weight ratio, resistance to corrosion and superior confinement through hoop action coming from the orientation of its constituent fibers (Hajsadeghi *et. al* 2010). FRPs also provide the advantage of easy and economical installation, although their manufacturing costs are much higher in comparison to steel. The inherent disparity in the mechanical properties and the associated costs of these different materials gives rise to a trade-off between cost and performance when it comes to retrofit operations. This study explores the aforesaid trade-off and aims to optimize bridge retrofit design configurations with respect to cost and resilience.

The study is a two-objective optimization problem that aims to minimize column jacket retrofit cost and simultaneously maximize the retrofitted performance measured in terms of bridge resilience. Multi-objective evolutionary algorithm, namely Non-dominated Sorting Genetic Algorithm II is used to carry out the optimization owing to its implicit elitism and simplicity in use. The variables in the parameter space include the choice of material for the retrofit, the choice of column in the bridge to be retrofitted and the thickness of the retrofit

material for each bridge column. Three different materials, steel, carbon fiber and glass fiber composites are investigated, each associated with different values of strength and unit cost. Required thickness of jacket and unit cost of jacketing differ for each material for the same target resilience. The algorithm hence, searches the domain to arrive at parameter values which are most favorable in terms of cost as well the resulting resilience of the retrofitted structure. Results from the optimization, called Pareto-optimal set, include solutions that are distinct from each other in terms of the associated cost, contribution to resilience enhancement, and values of design parameters. The user is offered a wide range of superior solutions to choose from, based on more specific preferences.

It is of interest to investigate seismic resilience enhancement due to column retrofit under the multi-hazard effect of earthquake and flood-induced scour in continuation to previous study by Prasad and Banerjee (2013). Hence the example bridge is evaluated for its seismic resilience for various retrofit configurations taking into account the bridge columns being exposed to pre-existing scour resulting in reduced structural stiffness.

TABLE OF CONTENTS

LIST OF FIGURES

LIST OF TABLES

ACKNOWLEDGEMENTS

Conducting thesis research has been a valuable learning experience in its entirety and I am most thankful to my advisor, Dr. Swagata Banerjee Basu, for her prompt guidance and encouragement without which I could not have overcome all the roadblocks in this pursuit. I extend my heartfelt thanks to my other committee member Dr. Maria Lopez de Murphy for her timely inputs and resources that proved invaluable with regard to the theoretical aspect of this research. Dr. Basu has been instrumental in getting past several challenges during the modeling phase of this project. Discussions with him on any aspect of this work have been most helpful and motivating.

I am grateful to my seniors Taner, Mehmet, Unmukt and Ashok for their patient help and well wishes throughout this study.

I sincerely acknowledge the partial financial support we were extended by the National Science Foundation (through Grant No. CMMI-1131359) and the Mid-Atlantic Universities Transportation Center (through Project No.PSU-2012-01).

Chapter 1

Introduction

1.1 Seismic Retrofit of bridge columns

Bridge performance is often controlled by the strength of its critical sub-structural components. The seismic response of highway bridges is governed significantly by the axial strength and ductility of its columns. Prior to 1971, bridge failures were often characterized by column failures at the plastic hinge zones due to poor detailing and insufficient confinement (Ramanathan 2012). The Caltrans Seismic Retrofit Program adopted the technique of column jacketing to provide the additional confinement required to restrict the lateral disintegration of column concrete. Steel jackets have been established as a means to increase the deformation capacity of the concrete beyond its unconfined compressive strength and consequently control the column rotational ductility under lateral loading. However, fiber reinforced polymer (FRP) is growing as a preferred alternative owing to its high strength to weight ratio, resistance to corrosion and superior confinement through hoop action coming from the orientation of the constituent fibers (Hajsadeghi *et. al* 2010).

Mander model originally developed to describe the behavior of concrete confined by transverse steel reinforcement has been widely used to characterize the stress-strain behavior of concrete confined by steel jackets (Mander *et. al* 1988). The Mander model was adopted to analyze FRP confined concrete until subsequent studies proved this use to be inaccurate owing to the elastic brittle nature of composite jackets as opposed to the ductile behavior of steel jackets (Saadatmanesh *et. al* 1994, Seible *et. al* 1995, Teng and Lam 2004). However in this study, the Finite Element model of the FRP retrofitted bridge column section is based on the Mander model.

In future study this may be modified to incorporate a more recent model namely the Teng and Lam model (Teng and Lam, 2004).

1.2 Multi-hazard scenario

Present civil engineering practice relies on individual hazard models to analyze natural and manmade hazards. Consequently, hazard mitigation techniques are developed based on structural failure probabilities under discrete hazard conditions. However, structures may be exposed to a variety of natural hazard conditions, including multihazard, during their service lives. Previous study demonstrated that among several possible combinations of extreme hazards, earthquake in the presence of flood-induced scour is a critical scenario for highway bridges located in seismically active, flood-prone regions (Prasad and Banerjee 2013). Seismic vulnerability analysis of typical California bridges pre-exposed to foundation scour resulting from various intensity flood events revealed significant deterioration of their seismic performance even under the effect of moderate scour (Banerjee and Prasad 2013). Flood induced scour on bridge piers has the effect of reducing structural lateral stiffness and consequently increasing the rotational response of the bridge columns under lateral loading. In this study it is of interest to investigate the effect of column jacket retrofitting in the scenario of increased bridge flexibility under the effect of pre-existing scour on pier bases.

1.3 Optimization problem

From more than a decade long research, confinement of bridge columns using wrap-around jackets has been established to have a positive impact on the seismic response of bridge structures owing to enhanced shear and flexural capacity of the columns (Priestley *et. al* 1996,

Haroun and Elsanadedy 2005). With the advent of displacement based seismic design in the early 1990s column jacketing has been widely adopted by several DOTs as a bridge rehabilitation and retrofit technique to ensure a ductile mode of failure in columns. Although steel has been the traditional choice of material for external confinement, the associated cost and time consumption in the installation process have led to exploring alternative lightweight materials with superior strength properties.

Fiber Reinforced Polymer composites were extensively being used in aerospace and shipbuilding before being applied for the first time for column wrapping by FYFE in the US in the1980s using carbon fiber (Priestley *et. al*, 1992). Bridge retrofit and rehabilitation is an integral part of highway bridge network maintenance. Today, with the variety of composite materials finding their place in the area of structural enhancement of bridges, it becomes relevant to the bridge owners and stakeholders to base their decisions regarding bridge retrofit on the relative cost-benefits of the various options laid out to them.

The inherent disparity in the mechanical properties and the associated costs of these different materials give rise to a trade-off between cost and performance when it comes to retrofit operations. This study explores the aforesaid trade-off and aims to optimize bridge retrofit design configurations with respect to cost and resilience.

The study is a two-objective optimization problem that aims to minimize column jacket retrofit cost and simultaneously maximize the retrofitted performance which is measured in terms of bridge resilience. Multi-objective evolutionary algorithm, namely Non-dominated Sorting Genetic Algorithm II is used to carry out the optimization owing to its implicit elitism and simplicity (Deb 2001, Deb *et. al* 2002). The variables in the parameter space include the choice of material for the retrofit, the choice of column in the bridge to be retrofitted and the thickness of the retrofit material for each bridge column. Three different retrofit materials, steel, carbon fiber and glass fiber composites are investigated, each with different values of strength and unit cost.

Required thickness of jacket and unit cost of jacketing differ for each material for the same target resilience. The algorithm hence, searches the domain to arrive at parameter values which are most favorable in terms of cost as well the resulting resilience of the retrofitted structure. Results from the optimization, are Pareto near-optimal solutions, that are distinct from each other in terms of associated cost, contribution to resilience enhancement, and values of design parameters namely, material properties and thickness of jacket. The user is offered a wide range of superior solutions to choose from based on more specific preferences.

A flow chart presented in Figure 1-1 shows the overall optimization process. The genetic algorithm treats every retrofit design parameter set (consisting of specifications for choice of material, thickness for each column) like an individual in the biological evolutionary process (Ferrolho and Crisostomo 2005). Every such 'individual' needs to be evaluated for its fitness based on which it either gets eliminated or is retained in the pool. Retained individuals generate 'off-springs' through recombination and mutation to keep the population pool replenished. The new population pool that includes both parents and off-springs is in turn evaluated and reduced; with every such cycle, the population fitness keeps improving due to elimination of unfit individuals and generation of fitter individuals.

Analogically speaking, the retrofit solution sets are the individuals generated by the algorithm which are incorporated into the bridge model. Nonlinear time history analyses are performed to generate bridge fragility information for resilience estimation of the bridge. The fitness of every parameter set is evaluated in terms of the two objectives i.e. seismic resilience and retrofit cost. Higher the retrofitted resilience and lower the cost, better is the fitness of the design parameter set.

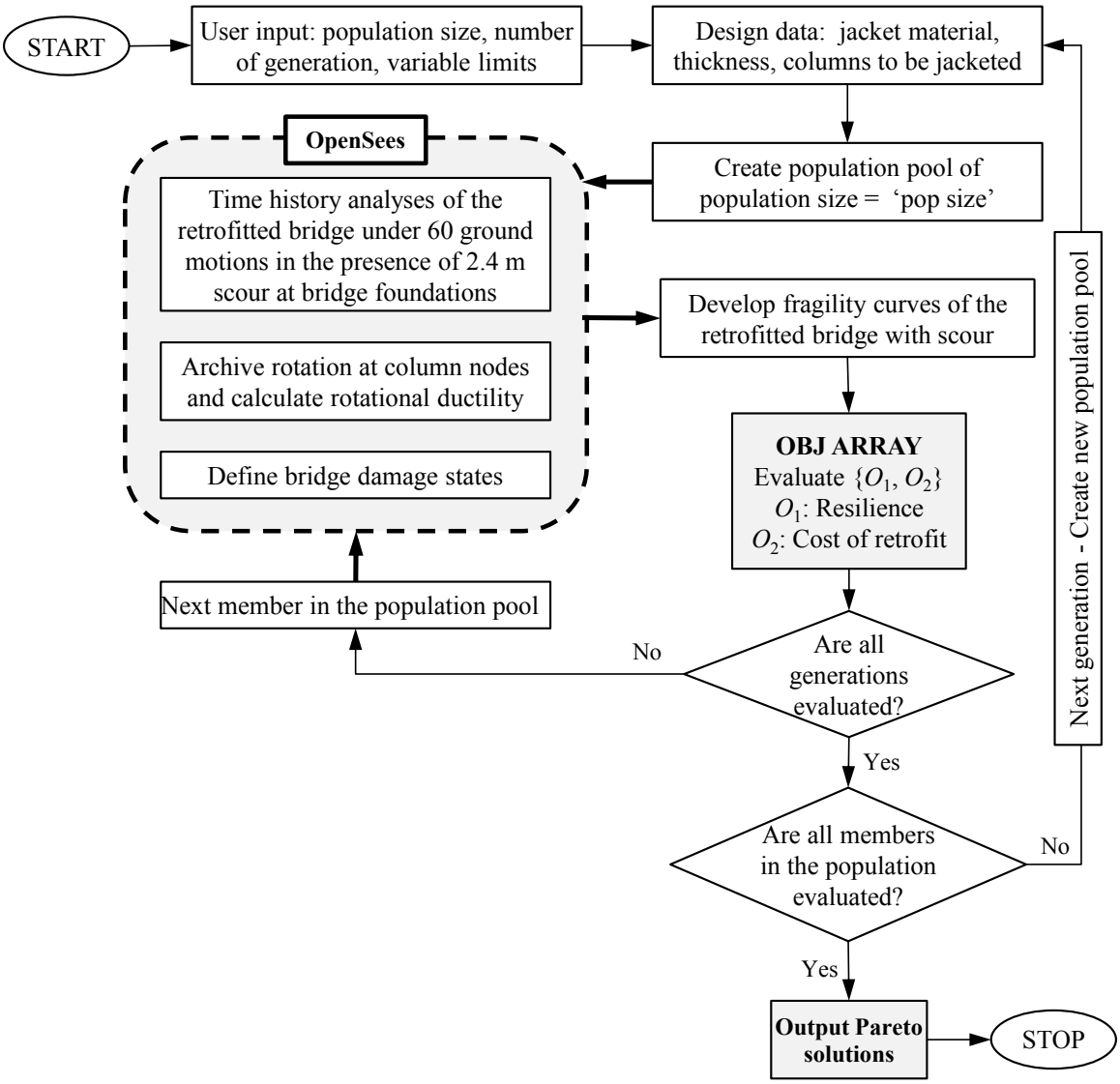

Figure 1-1. Flowchart of the optimization process

Chapter 2

Disaster Mitigation and Enhancement in Resilience through Retrofit Measures

Disaster resilience is defined by the National Academics as *the ability to prepare and plan for, absorb, recover from, and more successfully adapt to adverse events* (Cutter *et. al* 2013). It is also mentioned that *enhanced resilience allows better anticipation of disasters and better planning to reduce disaster losses—rather than waiting for an event to occur and paying for it afterward*. To achieve such enhancement in resilience, it is important that the post-event recovery of the affected system or society be successfully performed within an acceptable level of time and cost.

During the last decade, a paradigm shift has been observed in quantifying damage due to natural hazards to directly include socio-economic consequences that impact the concerned society (Zhou *et. al* 2010, Arcidiacono *et. al* 2012 and Venkittaraman and Banerjee 2013). Traditional approach to the design of engineered systems has implicitly been based on system resistance to an extreme event with certain probabilistic design magnitude. On the contrary, the new resilience-based design approach is a multi-parameter approach that accounts for the actual disaster phase as well as the post-event recovery phase of the system. It has been pointed out by Manyena (2006) that the traditional vulnerability based design model is *force based* whereas the resilience based design model is *time based.* Beyond just the estimation of damage due to the extreme event, resilience also incorporates the community preparedness to cope with a disaster in terms of its available resources to carry out mitigation operations.

For a single extreme event, system resilience can be analytically expressed as shown in Eq. (1) as (Cimellaro *et. al* 2010):

$$R = \int_{t_{0E}}^{t_{0E}+T_{LC}} \frac{Q(t)}{T_{LC}} dt \tag{1}$$

In the above expression, $Q(t)$ represents system functionality (expressed in the percentage scale), t_{0E} represents the time of occurrence of an extreme event E and T_{LC} is the control time set to evaluate resilience. Hence, higher the system resilience, higher is the area enclosed under the functionality curve between the time of occurrence of extreme event and the control time. The mathematical expression for $Q(t)$ as shown in Eq. (2) constitutes a loss function and a post-event recovery function during the period of system interruption due to the extreme event.

$$Q(t) = 1 - \left[L\left(I, T_{RE}\right) \times \left\{H\left(t - t_{0E}\right) - H\left(t - \left(t_{0E} + T_{RE}\right)\right)\right\} \times f_{rec}\left(t, t_{0E}, T_{RE}\right)\right] \tag{2}$$

$L(I,T_{RE})$ represents loss as a function of hazard intensity I and time of system recovery T_{RE}, and f_{rec} represents the post-event recovery function. $H(\,)$ is the Heaviside Step function that takes the value of zero for a negative argument and one for a positive argument. Similar definitions are used in literatures over a decade for the formulation of community resilience (Arcidiacono *et. al* 2010, Bruneau *et. al* 2003, Chang and Chamberlin 2004, Cimellaro 2013 and Paton and Johnston 2006), and evaluating the resilience of various lifeline systems such as acute care hospitals (Cimellaro *et. al* 2010), water supply systems (Rose and Liao 2005), power transmission systems (Shinozuka *et. al* 2004) and transportation systems (Amdal and Swigart 2010, Chang and Nojima 2001, Decò *et. al* 2013, Venkittaraman and Banerjee 2014)

In Eq. (2), the function $Q(t)$ would take the value 1.0 in the ideal cases of no damage or instant recovery. The corresponding resilience would then be 100 percent. Likewise, in the case of absolute shut down followed by no recovery, the functionality $Q(t)$ and consequently the system resilience would become zero. Therefore, resilience generally takes values in between 0 and 100 in real life scenarios and the value depends on both the degree of damage and the speed of recovery. Calculation of resilience requires estimation of its two components, the loss and the recovery functions. The following sub-sections describe the loss and the recovery models adopted in this study.

2.1 Loss model

Figure 2-1 shows the loss and recovery phases of the functionality of a system both of which account for the estimation of its disaster resilience. Losses due to a natural disaster constitute (i) direct loss, that represents the cost associated with post-event structural system restoration and (ii) indirect loss that relates to all the socio-economic disruptions arising during the period of system restoration.

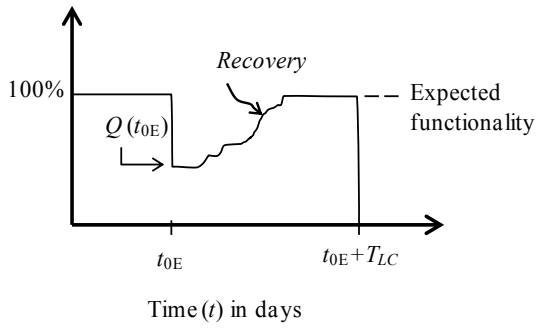

Figure 2-1. Schematic representation of loss and post event recovery functions

2.1.1 Direct losses

Direct loss is related to system performance during the extreme event, and hence is estimated based on the structural damage of the system due to the event. For highway bridges, the direct loss estimation methodology prescribed by HAZUS (HAZUS –MH MR5) makes use of bridge vulnerability model, expressed in the form of fragility curves. *Fragility curves are functions that represent the probability that the response of a specific structure exceeds a given performance threshold associated with a performance limit state, conditional on earthquake intensity parameter I, such as peak ground acceleration* (Cimellaro *et. al 2010*). The aforesaid performance limit states refer to the level of damage that may be reached by the affected structural system based on its vulnerability. These are categorized into minor, moderate, major or collapse. Analytically, fragility function for a given damage state *k* may be represented as

$$F(PGA_j, c_k, \zeta_k) = \phi\left(\frac{\ln\left({}^{PGA_j}/_{c_k}\right)}{\zeta_k}\right) \tag{3}$$

In the above expression, PGA_j refers to the given earthquake intensity in terms of its peak ground acceleration, c_k is the median value or the PGA corresponding to 50% probability of exceedance of the damage state k, and ζ_k is the log-normal standard deviation which determines the dispersion of the fragility curve. ζ_k is taken as 0.5 for all the damage states as per the recommendations of HAZUS (1999) based on the studies performed by Pekcan (1998).The fragility parameter c_k is determined by maximization of the likelihood function given as

$$L = \prod F(PGA_j, c_k, \zeta_k)^{r_j} 1 - F(PGA_j, c_k, \zeta_k)^{1-r_j} \tag{4}$$

In Eq. (4), r_j takes the value 1 if the damage state k was attained and 0 if otherwise. Fragility functions developed based on Eq. (3) for each damage state provide the information (in the form of probability of exceedance) necessary to estimate direct economic loss. Direct economic loss L_D is expressed in terms of ratio of bridge restoration cost C_{rE} to replacement cost C given as

$$L_D = \frac{C_{rE}}{C} = \sum_k P_E(k) \times r_k \quad (5)$$

As shown in Eq. (5), for a given seismic event E, direct economic loss is calculated as the sum of the products of the damage ratio r_k and the probability of exceedance $P_E(k)$ for each damage state k. $P_E(k)$ at each state is obtained from the corresponding fragility curve and the damage ratios are based on the recommendations by HAZUS (1999) as shown in Table 2-1. This approach for direct loss estimation of highway transportation systems due to seismic damage is well adopted in previous studies (Zhou *et. al* 2010, Banerjee and Prasad 2013, Venkittaraman and Banerjee 2013). The same approach is followed in the present study for the evaluation of direct loss.

Table 2-1. Damage ratios as per HAZUS (1999)

Damage State	Damage ratio
Minor	0.03
Moderate	0.08
Extensive	0.25
Collapse	2/n, n is the number of bridge spans

2.1.2 Indirect losses

While direct losses as defined by HAZUS-MH (2003) are simply the costs required to repair a bridge structure back to its 100% capacity after incurring damage due to an earthquake event, indirect losses are calculated based on the drop in the entire transportation network performance. Indirect losses are associated with the prolongation in travel time due to detours, increased vehicle operational costs, risk of accidents and the lack of opportunity to carry out economic activities due to the inability to travel. The calculation of indirect costs due to a seismic failure therefore necessitates the consideration of a highway network with known characteristics such as its traffic flow data, location and orientation of the network bridges and distance between various source and destination nodes, which are beyond the scope of this study. In the retrofit cost benefit study performed by Dennemann (2009) the indirect losses due to bridge seismic failures were shown to be in the range of 5 – 20 times the direct economic losses. In this regard, Venkittaraman and Banerjee (2013) demonstrated that the seismic resilience of a highway bridge is not sensitive to the indirect to direct loss ratio when varied from 5 to 21. It is recognized, however, that this ratio could be less than 5 or greater than 21 based on the region, the accessibility and importance of the highway corridor to the local population in which case there may a different impact on system resilience. The present study adopts an expected value of 13 for this ratio although the extreme cases are examined individually to observe the sensitivity of bridge fragility curves to the indirect to direct loss ratio.

Total loss inclusive of both direct and indirect losses is incorporated into resilience estimation in Eq. (2) as the loss function $L(I, T_{RE})$. Total loss function is given by the ratio of total repair cost to total replacement cost as shown in Eq. (6):

$$L(I, T_{RE}) = \frac{L_D + 13L_D}{1 + 13L_D} \tag{6}$$

2.2 System recovery

The duration and pace of a bridge restoration process is highly dependent on the disparity existing between the extent of damage and the preparedness of the community to drive the recovery. Accurate simulation of the path of recovery becomes challenging in the absence of event or location specific information. In this regard, Cimellaro *et. al* (2010) proposed simplified modeling of bridge functionality during recovery using different mathematical functions namely, linear, exponential and trigonometric as shown in Figure 2-2. Exponential function simulates the scenario that abundant resources for repair are readily available to instantly initiate recovery, whereas a trigonometric function models the case where the pace of recovery is slow initially and picks up with time. Based on the study of real-time bridge recovery processes Zhou *et. al* (2010) recommend the use of a linear recovery function which is being adopted in this study, considering the lack of further information on the community response.

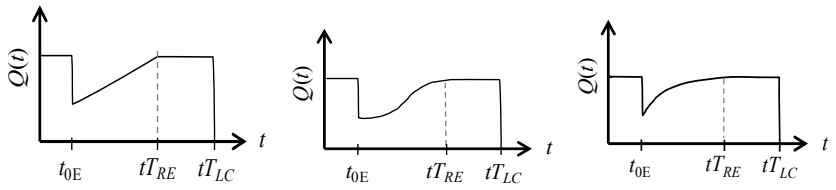

Figure 2-2. Recovery functions (a) Linear (b) Trigonometric (c) Negative exponential.

2.3 Seismic hazard model

Seismic fragility analysis of the bridge is conducted using a suite of sixty ground motion time histories with peak ground acceleration values ranging from 0.1g to 0.3g. This suite developed by Federal Emergency Management Agency (FEMA) for the Los Angeles region in

California, consists of both recorded and synthetic ground motion histories with exceedance probabilities 2%, 10% and 50% in 50 years. Each of these three sets consists of 20 ground motion histories.

Bridge seismic damage in this study is characterized by flexural and shear failures at the piers only, for various cases of column retrofitting. Other modes of bridge failure such as girder unseating and foundation failure are assumed to be non-governing. In order to develop bridge fragility curves for the considered modes of failure it is necessary to quantify seismic damage at the piers in terms of discrete damage states namely minor, moderate, major and collapse. Shear failure being brittle and sudden is taken as collapse state whereas flexural damage is evaluated based on rotational ductility of the piers. Rotational ductility is defined as the ratio of response rotation to rotation at yield ($(= \phi/\phi_y$).

During earthquake time history analysis the maximum rotational ductility for each pier is calculated by dividing the highest recorded rotation by yield rotation obtained from section moment-curvature analysis plots as shown in Figure 3.4. The rotational ductility so obtained is used to identify the bridge damage state by comparing against certain pre-defined threshold limits. These threshold limits of rotational ductility for each damage state are obtained using the drift limits set by HAZUS (1999) as shown in Table 2-2.

Table 2-2 Drift ratios and threshold values of ductility

Damage states	Non-seismic drift ratios (HAZUS 1999)	Threshold rotational ductility for unretrofitted column
No damage	0.005	1.00
Minor	0.01	1.51
Moderate	0.025	3.04
Major	0.05	5.60
Collapse	0.075	8.15

Chapter 3

Example Bridge Model

3.1 Bridge schematic

For the purpose of this study the five span example bridge model developed by Sultan and Kawashima (1993) was adopted, which was designed in accordance to the seismic design specifications made by California Department of Transportation (Caltrans). As shown in the bridge schematic in Figure 3-1 the prestressed box girder is 2.13 m deep and 12.95 m wide and is continuous over four circular single column bents which are identical in length (19.8 m) and diameter (2.4 m). The span configuration is such that the two end spans are 39.6 m long and the three middle spans are each 53.3 m long. Each column is monolithically connected to the girder at the top and is resting on a single, large-diameter, 18.3 m-long augered pile (with same diameter as the pier) fully fixed at the base. Such large-diameter pile (extended column) foundations are increasingly being used by several state DOTs under high lateral and seismic load demand. Cross-sectional properties of these piles are identical to those of the column section.

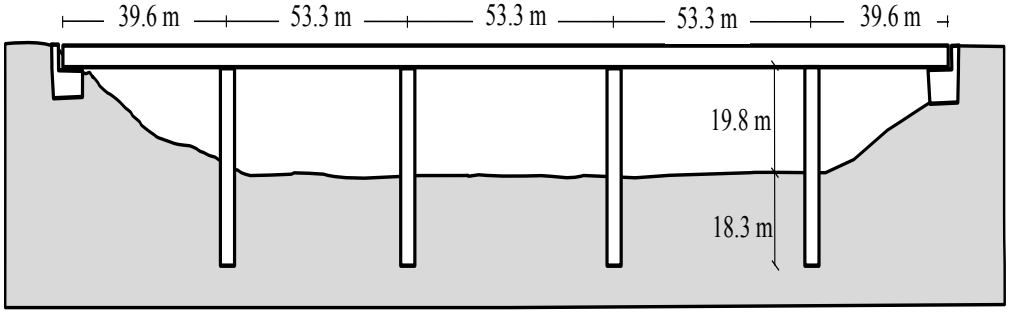

Figure 3-1. (a) Schematic of example bridge model in elevation

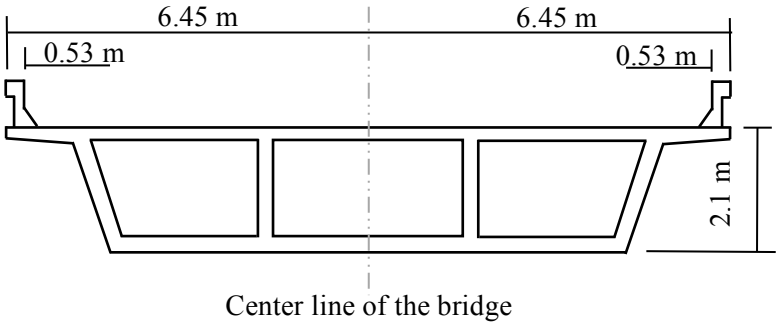

Figure 3-1. (b) Box girder section

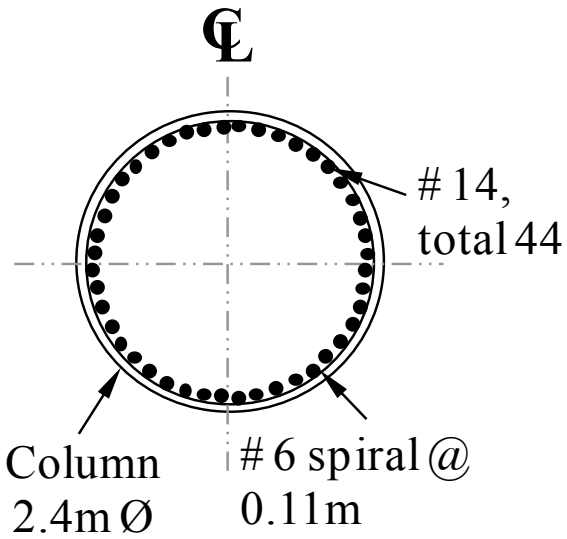

Figure 3-1. (c) Column cross-section

Figure 3-1. Schematic of example bridge model (a) Bridge elevation, (b) Box girder section and (c) Column cross-section

3.2 Modeling of bridge components

Three dimensional finite element model of the example bridge was developed and analyzed for seismic loading in the software platform *OpenSees* (McKenna and Fenves 2012).

During seismic loading, the girder is expected to behave like a perfectly elastic rigid body and is modeled using linear elastic beam elements with lumped stiffness properties. The monolithic beam-column connection is simulated by modeling the connecting element between girder and column as a rigid link, with the two end nodes having equal displacements in all degrees of freedom. Bridge columns and mono-piles are all modeled using displacement-based fiber elements whose cross-sections are meshed in the manner as shown in Figure 3-2. Fully fixed boundary condition is assigned to each pile base.

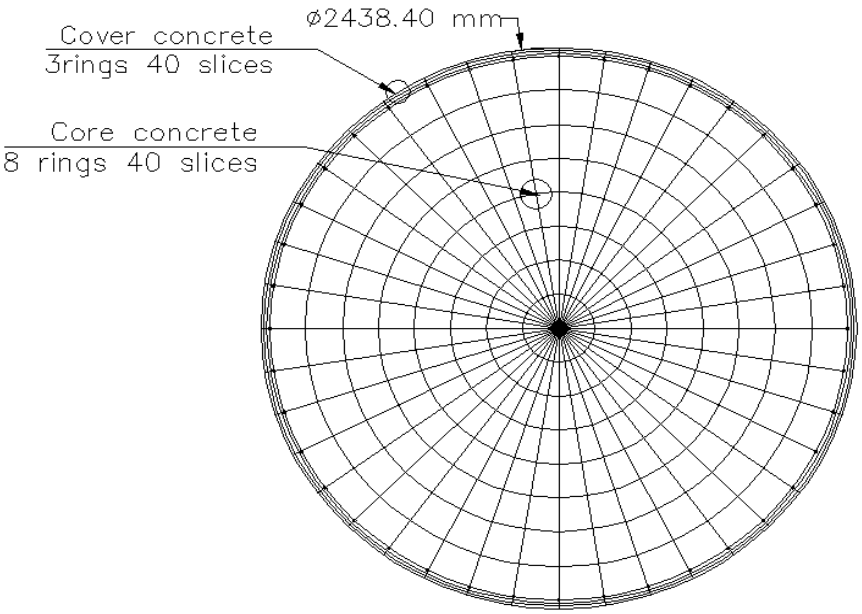

Figure 3-2. Column section fiber elements

3.3 Material model

In OpenSees, the material models *Concrete02 and Steel02* are used to model the column concrete and reinforcing steel fibers, respectively. However, jacket confined column section (both steel and FRP jackets) is modeled using the *ConfinedConcrete01* material which is based on Mander's confined concrete model.

3.3.1 Material model validation

In order to validate the *ConfinedConcrete01* material model, stress strain plots are obtained in OpenSees for compressive loading of small circular cylinder models (6 in. by 12 in.) up to failure, for various layers of composite wrapping. These plots are compared against experimental stress-strain relations obtained from CSUF (2003). California State University, Fullerton (CSUF) studied the enhancement of axial loading capacity of cylinder specimens wrapped with 1, 2 and 3 layers of *Tuflam* carbon/epoxy composite systems under uniaxial compression. The mechanical properties of the laminate as obtained from the CSUF test data are shown in Table 3-1. The stress-strain relations based on OpenSees simulation, for the same three cases of retrofit (1, 2 and 3 layers of *Tuflam –C* laminate) are shown in Figure 3-3. Table 3-2 shows the comparison between the experimental and simulation test results in terms of ultimate stress and strain. It is observed that the error between the computational and experimental ultimate stress values increases with the number of plies applied. The disparity could be due to the fact that the OpenSees *ConfinedConcrete01* material behaves as per the Mander model (1994) while the experimental results would be better characterized by a model that takes into account brittle failure of jacket. Also, *OpenSees* takes the ultimate strain value from the user as one of the

parameters for defining a *ConfinedConcrete01* material, which would certainly affect the slope of the post-yield stress-strain curve.

Table 3-1 Mechanical properties of *Tuflam-C* from CSUF report (2003)

System	Thickness inch (mm)	Ultimate strength ksi (MPa)	Strain at ultimate	Modulus of elasticity ksi (GPa)
Tuflam -C	0.04 (0.84)	154 (1061)	0.012	14000 (96.5)

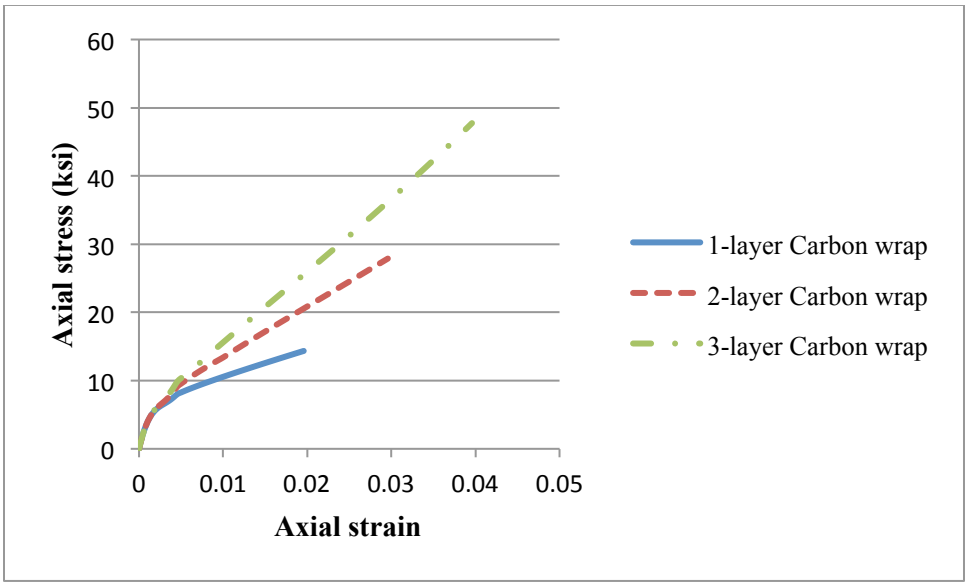

Figure 3-3. Axial stress strain curves obtained from *OpenSees*

Table 3-2 Comparison between computational and experimental stress-strain values

Number of plies	*OpenSees* ultimate stress (ksi)	Experimental ultimate stress (ksi)	*OpenSees* ultimate strain	Experimental ultimate strain
1	13.9	9.54	0.018	0.012
2	27.0	15.0	0.030	0.030
3	44.0	19.0	0.040	0.017

3.4 Mechanical properties of chosen retrofit materials

It is of interest to formulate a multi-objective optimization problem to understand the relative cost-benefit of different retrofit materials. In this regard, A 36 steel is chosen for the steel jacket retrofit case whereas in the case of composites, carbon and glass fabrics namely TU27C and VU27G manufactured by *Quakewrap Inc.* were adopted. These are both high-strength unidirectional fabrics whose material properties as obtained from *Quakewrap* product datasheets are shown in Table 3-3.

Table 3-3 Mechanical properties of *Quakewrap* composite laminates

Product	Tensile strength (ksi)	Tensile modulus (ksi)	Ultimate elongation	Ply thickness (inch)
TU27C laminate	135	13000	0.98%	0.049
VU27G laminate	85.2	3980	2.3%	0.05

In the optimization process, one of the objectives is to minimize the cost of retrofit. Although retrofit cost-benefit assessment is performed considering service lives of the retrofitted bridges, in practice, the initial investment or the manufacturing cost is one of the governing factors in the decisions made regarding retrofit design. It is a well-known fact that composites are a much more expensive alternative to steel in terms of material. However, their high strength to

weight ratio makes them drastically quicker and economical as far as installation is concerned. Therefore, the results from the optimization vary significantly based on the type of expenses being incorporated. In the present study, retrofit design cost is evaluated in terms of material consumption only. Thus, in order to calculate the cost objective in the optimization study, the unit costs of the composite fabrics were obtained from the manufacturers as $9.84 and $2.94 per sq. ft for TU27C and VU27G sheets respectively. Unit cost of jacket steel is taken at a typical market value of $500 per ton.

3.5 Bridge fragility curves

In order to illustrate the comparison between the various retrofit materials in terms of their impact on bridge vulnerability, fragility curves are developed for the bridge model retrofitted with 0.5 inch thick jackets of each material. Thickness value of 0.5 inch is chosen, considering the reasonable lower limit for steel jackets. A separate moment-curvature analysis was performed for each case in order to obtain the yield and ultimate rotation values necessary to develop the fragility curves. Figure 3-4 shows the moment curvature plots for an unretrofitted bridge column as well as columns retrofitted with 0.5 inch thick jackets made of steel, carbon/epoxy and glass/epoxy laminates. The rotational ductility values indicated on each of these plots reflect the respective effectiveness in improving bridge resilience. The unretrofitted column section has a base ductility of 8.84, which is nearly quadrupled in the case of carbon/epoxy composite jacket. Steel and glass/epoxy yield comparable improvement in the ductility ratio to 20.4 and 22.2 respectively.

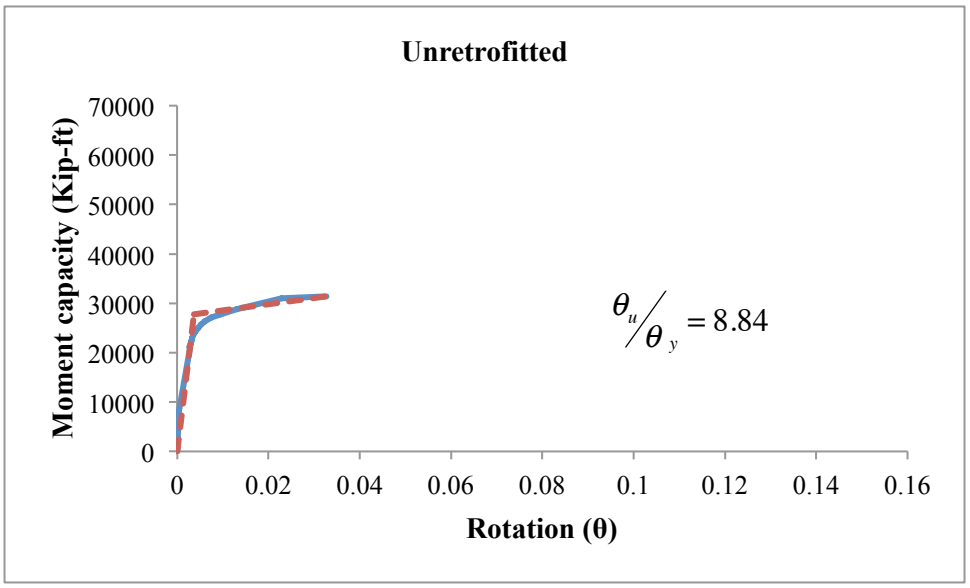

Figure 3-4 (a). Moment capacity - curvature plot for unretrofitted column

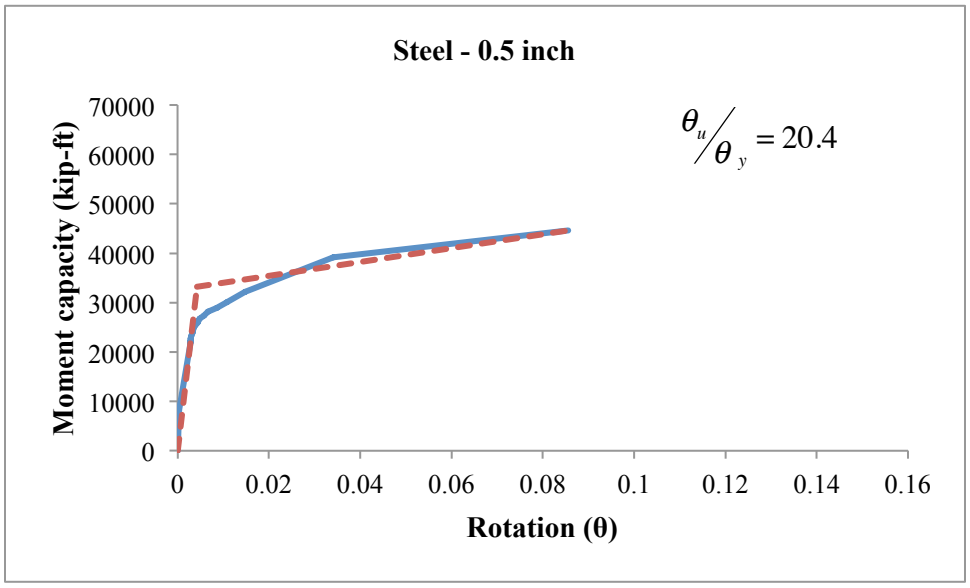

Figure 3-4 (b). Moment capacity - curvature plot for 0.5 inch steel jacketed column

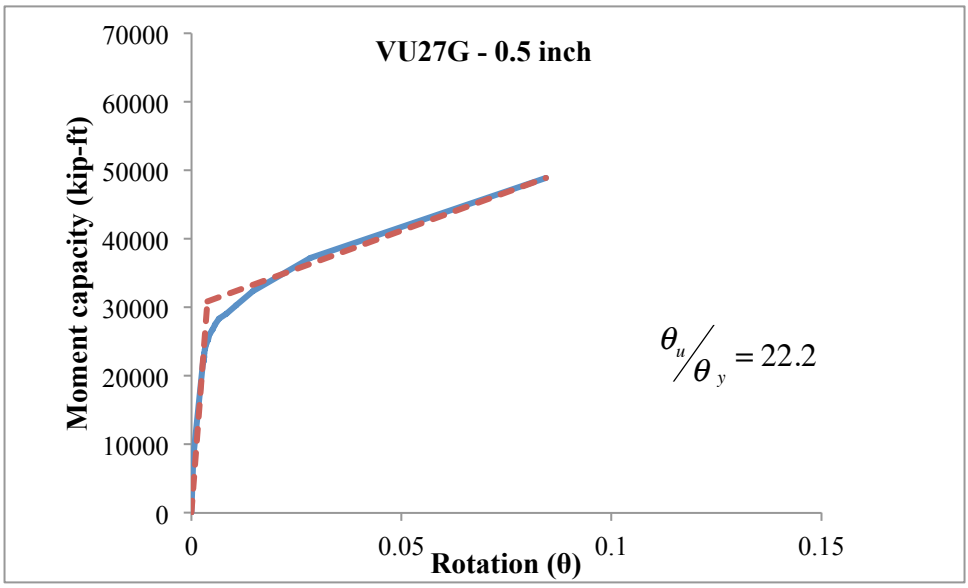

Figure 3-4 (c). Moment capacity - curvature plot for 0.5 inch VU27G jacketed column

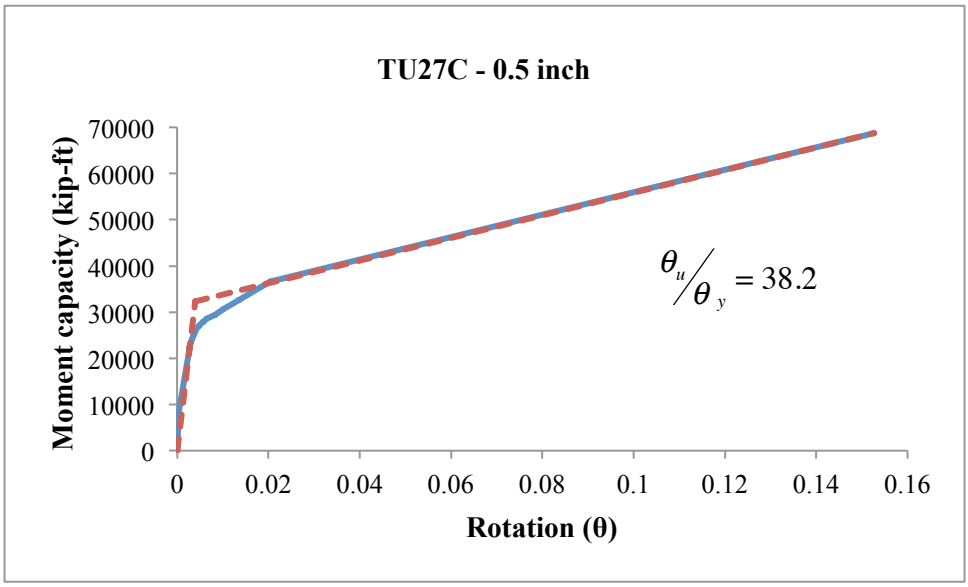

Figure 3-4 (d). Moment capacity - curvature plot for 0.5 inch TU27C retrofitted column

Figure 3-4. Moment capacity-curvature plots

Figure 3-5 shows the fragility curves and resilience values corresponding to the above moment – curvature plots. Predictably, the resilience values for the above four cases show the

same trend as the rotational ductility values i.e. for the same jacket thickness, TU27C enhances resilience by the largest extent from the base value of 57.7% corresponding to unretrofitted case, to 82.6%. Probability of higher damage states namely major and collapse reaches zero for this case of retrofit at least for ground motions with PGA values up to 1.5g.

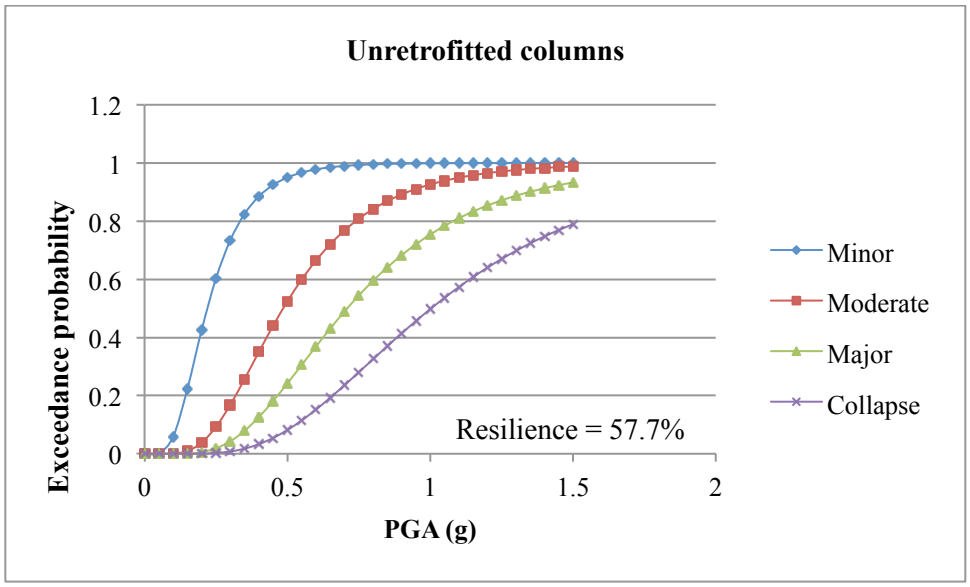

Figure 3-5 (a)

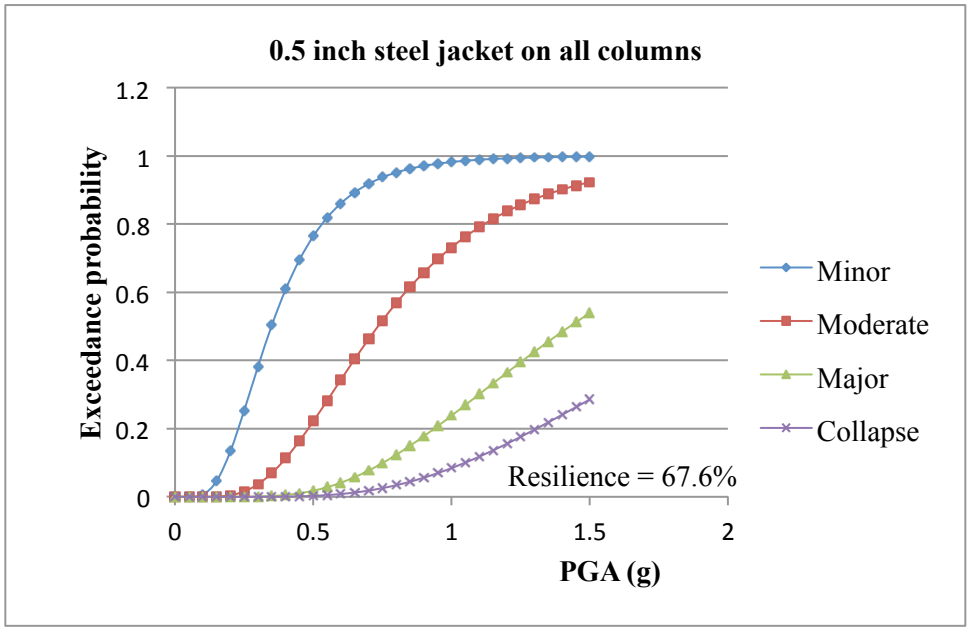

Figure 3-5 (b)

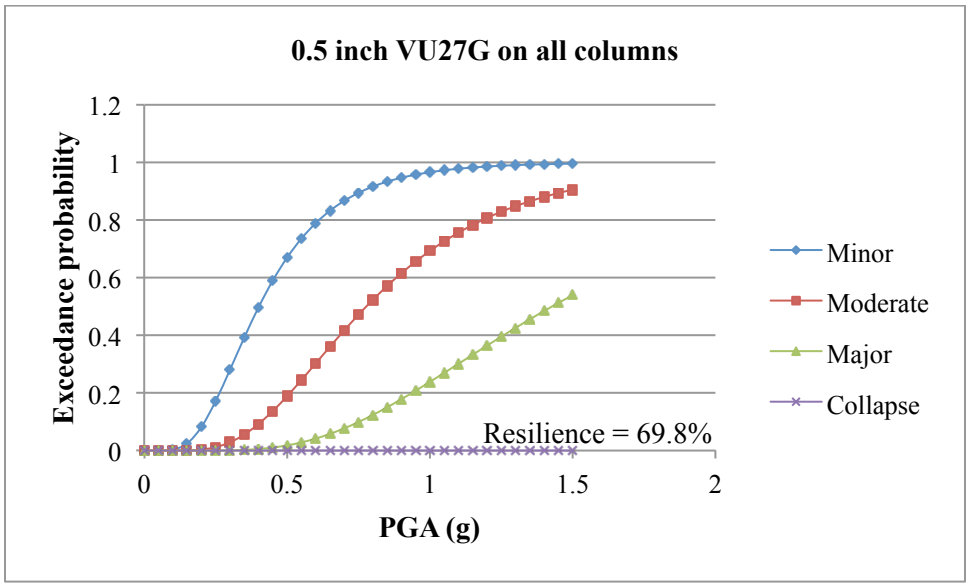

Figure 3-5 (c)

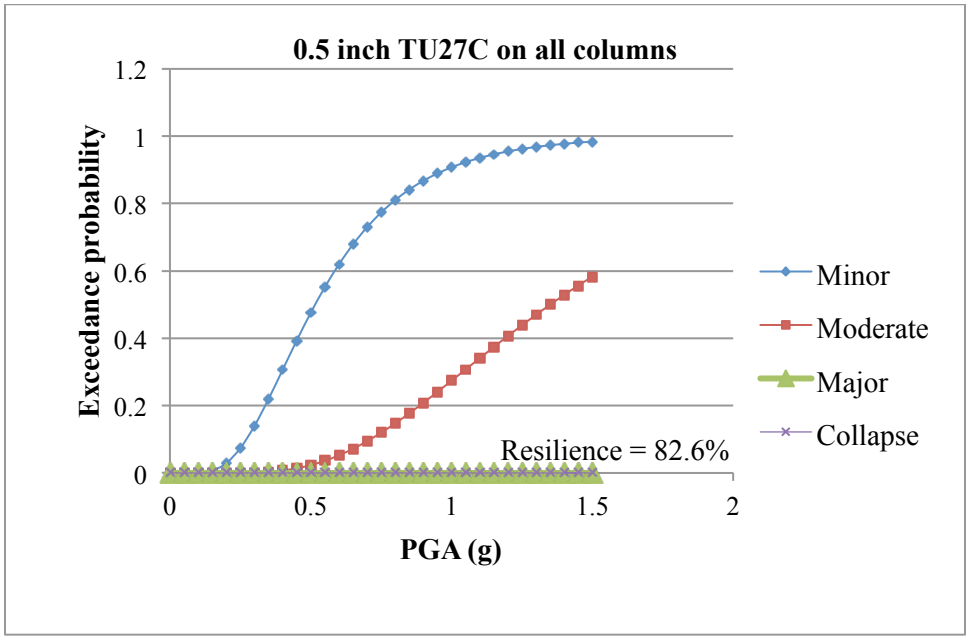

Figure 3-5 (d)

Figure 3-5. Fragility curves (a) Unretrofitted (b) 0.5 inch steel jacket on all columns (c) 0.5 inch VU27G on all columns (d) 0.5 inch TU27C on all columns

Chapter 4

Multi-Objective Optimization Analysis and Results

4.1 Pareto optimality

In any multi-objective problem, the presence of conflicting objectives implies that there is no single best solution, but a suite of solutions in which none can be explicitly said to be superior to any other in the absence of further information on preference. Multi-objective evolutionary algorithms offer an efficient and effective means to obtain a "Pareto near-optimal" set of solutions. These solutions, collectively known as Pareto front, are superior to every solution outside of their set but cannot dominate each other on one objective without becoming inferior on another. This concept is demonstrated in Figure 4-1, which corresponds to a problem that minimizes both objectives 1 and 2.

NSGA II groups solutions into different 'fronts' based on their ranking. In the figure, solutions belonging to the same rank (or front) are represented by the same shape (circles, triangles or diamonds). All solutions represented by circles have better fitness than the 'triangles' and the 'diamond', since they hold lesser values on both the axes (minimization problem). Likewise, solutions on front 2 (denoted by triangles) are fitter than that on front 3 (diamond). It should be noted that every 'circle' is better than every other 'circle' in terms of one and only one objective. These are not clearly superior to one another and are hence similarly ranked. Such a group would form a Pareto front. As the search progresses, the fitness of the solutions would improve and the fronts would get closer and closer to the origin. However, since our problem is aimed at minimizing one objective i.e. cost, and maximizing the other i.e. resilience, the 'sweet-

spot' region is located on the right side bottom of the graph if the resilience and cost objectives are defined on the horizontal and vertical axes respectively.

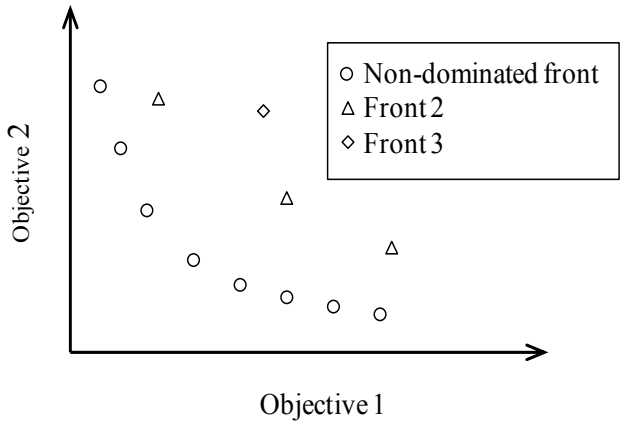

Figure 4-1. Pareto optimality

4.2 Optimization problem statement

The optimization problem is formulated as follows.:

Maximize: **Resilience (m, t_1, t_2, t_3, t_4)**,

Minimize: **Retrofit cost (m, t_1, t_2, t_3, t_4)**,

m Є {1,2,3}

t_1, t_2, t_3, t_4 Є [1 10 layers], for m={2,3}

t_1, t_2, t_3, t_4 Є {3/8", ½", ¾", 1"}, for m={1}

Where,

m is the material tag = 1, 2, 3 for steel, TU27C and VU27G respectively, and

t_1, t_2, t_3, t_4 are thicknesses of jackets (in inches if steel jacket and number of plies if composites) applied to columns 1, 2, 3 and 4 respectively.

4.3 Analysis using all three retrofit materials

Based on preliminary sensitivity analyses it was observed that for a population size of 20, convergence was attained within 25 maximum generations. Hence, this configuration was adopted for the final run. The variation parameters namely, the mutation and recombination ratios were kept at a recommended value of 0.4 (given by $^{2}/_{number\ of\ variables}$) (Song 2011). Among all the generations, results from only the 1st, 5th, 10th, 15th, 20th and 25th are presented in Figure 4-2. Also, for the final generation, the Pareto near-optimal retrofit configurations are presented in Table 4-1 in the increasing order of resilience (and cost, since they are non-dominated solutions of the same front). From Figure 4-2 it can clearly be seen that, at generation-15, all the Pareto solutions have already nearly reached convergence. Moreover, the solutions are well distributed between the lowest and highest attainable values of resilience (57% and 82% corresponding to unretrofitted and maximum retrofit cases respectively) indicating exhaustiveness in search.

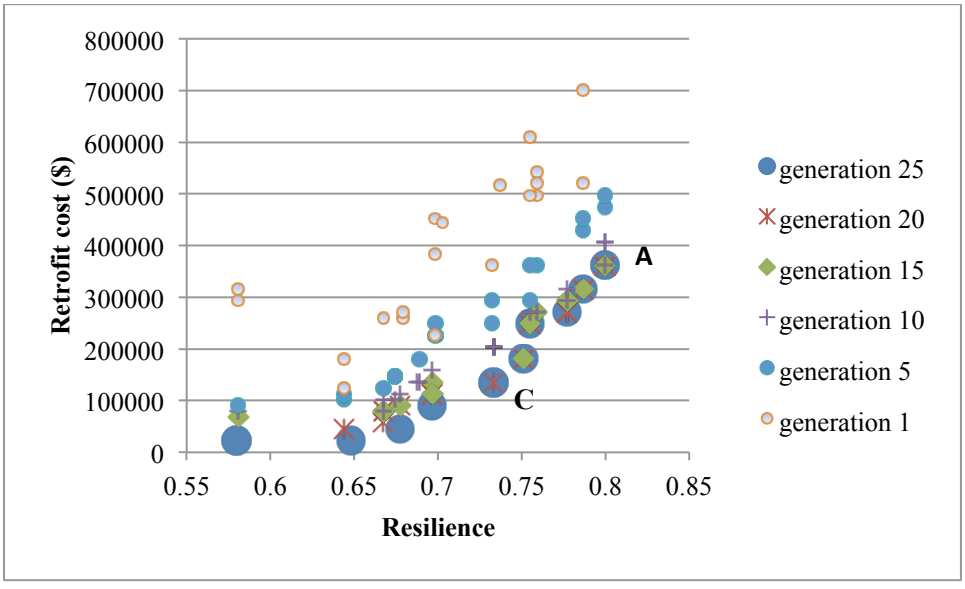

Figure 4-2. Final generation Pareto fronts

Table 4-1 Final generation Pareto fronts

Material	Number of layers				Resilience (%)	Cost($)	Resilience to cost ratio ($\times 10^3$)
	Column 1	Column 2	Column 3	Column 4			
TU27C	0	1	0	0	57.9	22598	2.56
VU27G	0	1	1	0	64.7	22663	2.85
TU27C	0	1	1	0	67.8	45195	1.50
TU27C	0	2	2	0	69.6	90391	0.77
TU27C	0	3	3	0	73.3	135588	0.54
TU27C	0	4	4	0	75.1	180784	0.42
TU27C	1	4	4	2	75.5	248577	0.30
TU27C	0	6	6	0	77.7	271175	0.29
TU27C	1	6	6	1	78.6	316371	0.25
TU27C	1	7	7	1	79.9	361567	0.22

Some redundancy in the solution set is observed owing to the inherent symmetry in the bridge, giving rise to identical results for symmetric retrofit configurations. Steel has been eliminated from the solution pool even in the early stages of the search possibly due to the imbalance against the large number of composite retrofit options to choose from. The course of the search over regular intervals has been tracked and presented in Figure 4-3 to understand the elimination of the glass/epoxy and steel jacket solutions. Based on Figure 3-5 (c) it can be seen that for a glass/epoxy jacket even as thick as 0.5 inch bridge resilience does not reach 70%. Hence the generated glass/epoxy optimal solutions (represented by squares in Figure 4-2) lie in the neighborhood of 65% resilience, closely competing with neighboring TU27C solutions that yielded marginally better resilience at the same cost, as can be observed at generations 15 and 25. The only solution that survived till the last generation (marked as ‘1’) is the one that yielded a resilience of 64.7% at $22663 which is half the cost as compared to the neighboring TU27C solution that yielded 67.7% at $45195 (marked as ‘2’).

On the other hand steel jacketing solutions generated in generation-1 got subsequently replaced by a TU27C solution of the same resilience at a better cost (lying vertically below them on the graph at generation-1).

Based on the optimal retrofit configurations it may be safely inferred that jacketing is effectively restricted to the internal columns that appear to significantly alter the bridge flexural response and in turn impact the resilience. The best performing non-dominated solution on the resilience axis yielding nearly 80% (marked as 'A') corresponds to 7 layers of carbon/epoxy jacketing around the middle columns with 1 layer each on the exterior columns. This is very close to the 82% resilience obtained using 0.5 inch thick jacketing (more than 12 layers) as was shown in Figure 3-5 (c). In fact from Table 4-1, in the zone of 80% resilience the most economical solution choice would be the 6-layer configuration around the middle columns without any jacketing around the exterior columns. However, the best compromise between the two objectives could be struck at 3-layer jacketing of interior columns in the 75% resilience range considering the disparity between neighboring solutions (solution marked as 'C').

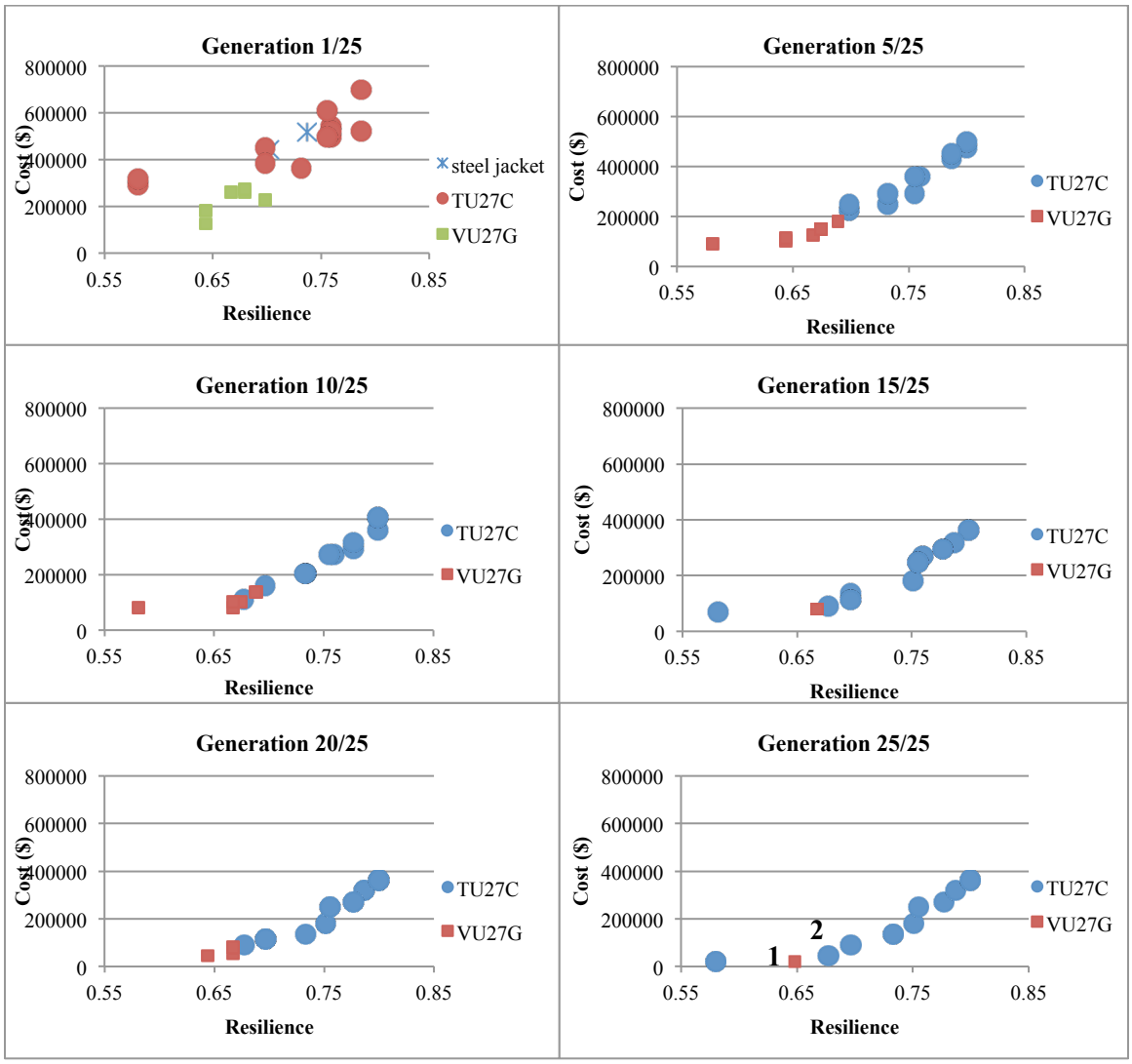

Figure 4-3. Tracking the final run analysis at every 5th generation

4.4 Optimization run II with only GFRP options

A separate analysis was set up to find optimal jacketing configurations using the glass/epoxy composite, VU27G only. The population size was kept at 26 and the maximum number of generations at 35 based on preliminary sensitivity analysis. The final generation solution set consists only of 13 unique solutions due to redundancy, indicating that the convergence was not pre-mature. Also, based on Figure 4-3 which shows Pareto fronts at

different instants during the search, it is evident that the convergence has been achieved by the 15th generation itself, indicating that the chosen maximum number of generations was reasonable. Table 4-2 summarizes the final generation optimal retrofit configurations from run II.

The algorithm recognizes the symmetry of the bridge during the course of the search, which is evident from the increasing occurrence of symmetric retrofit solutions. The interior columns are invariably more heavily jacketed suggesting their significant participation in bridge flexural behavior. In Figure 4-4 it can be observed that as the search progresses, the solutions are favorably shifting rightward and downward indicating enhancement on the resilience axis and deterioration on the cost axis. The solution indicated with the tag '4' is the best compromise solution as it increases resilience to 66.7% from 57.7% given by solution '1', by quadrupling the cost. On the other hand, the resilience can only be marginally improved to 67.5% as shown by solution '8' using six times the cost of solution '1'. In the neighborhood of the highest resilience value of 70.2%, solution '7' outperforms '2' as it offers practically the same resilience (69.4%) with a cost saving of $100000. It translates into saying that retrofitting the interior columns with more than 6 layers does not yield a benefit on resilience in good proportion to the additional cost investment.

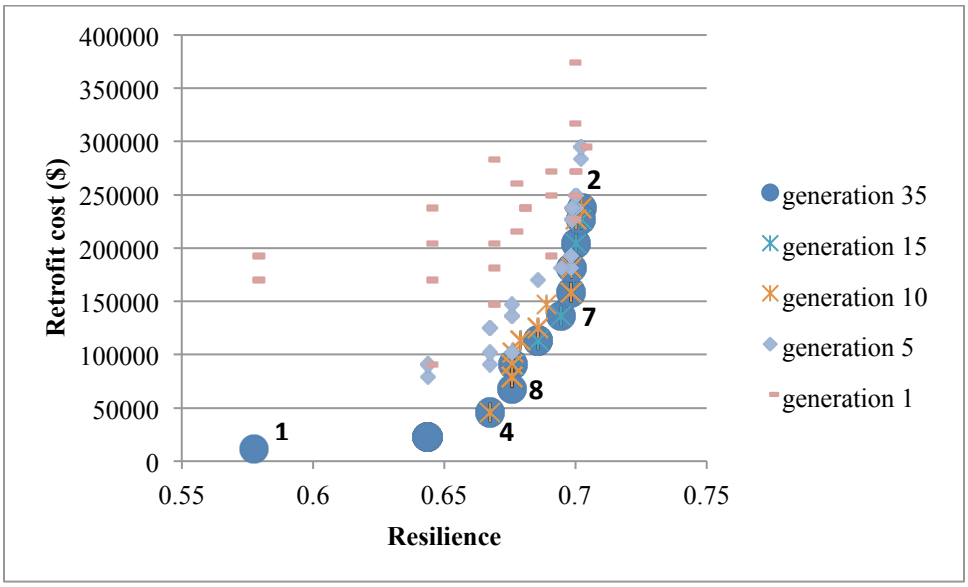

Figure 4-4. Glass/epoxy run Pareto fronts

Table 4-2 Glass/epoxy run Pareto fronts

S.No	Number of layers				Resilience (%)	Cost ($)
	Column 1	Column 2	Column 3	Column 4		
1	0	1	0	0	57.7	11331.6
2	0	10	10	1	70.2	237964
3	0	1	1	0	64.3	22663.3
4	0	2	2	0	66.7	45326.5
5	0	4	4	0	67.6	90653.1
6	0	5	5	0	68.5	113316
7	0	6	6	0	69.4	135980
8	0	3	3	0	67.5	67989.8
9	1	6	6	1	69.8	158643
10	1	8	8	1	70.0	203969
11	1	7	7	1	69.8	181306
12	1	9	9	1	70.2	226633
13	0	1	1	0	64.3	22663.3

4.5 Optimization run III with only steel jacket options

In run III, steel jacket configurations were explored separately, using a population pool of size 20 and 35 maximum generations. The Pareto fronts are shown in Figure 4-5. The optimization input domain includes three realistic options for the jacket thickness namely, 3/8 inch, 1/2 inch, 3/4 inch and 1 inch.

The solutions do not form well-defined Pareto fronts due to the existence of a clearly dominating single solution. The best compromise solution is the one with the retrofit configuration of 3/8 inch jackets around the middle columns only (indicated by '1'). The 1st generation solution (indicated by '2') with thicker jackets on the interior columns (3/4 inch and 1 inch) and additional jackets on the exterior columns does not yield any higher resilience whatsoever in comparison to solution '1'. This not only indicates the extraneousness of jacketing the exterior columns as inferred previously, but also points out the low sensitivity of resilience to increasing jacket thickness from 3/8 inch to 1 inch. Although better resilience may be achieved using higher thickness, the mentioned configuration is the single optimum solution for the given design parameter domain.

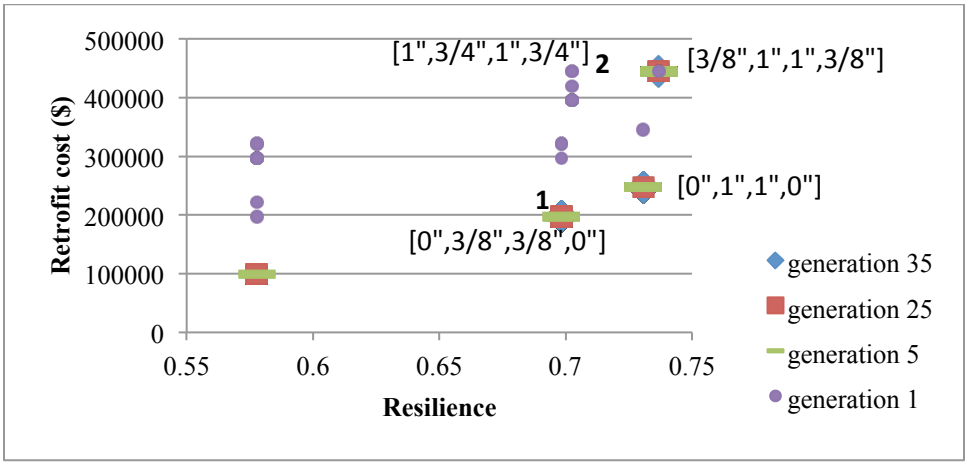

Figure 4-5. Steel jacket run Pareto fronts

4.6 Partial jacketing options

It is of interest to investigate the effect of partial column jacketing on bridge seismic resilience, in order to test the possibility of including length of jacket as an optimization variable. In order to identify the most critical region on the column to be jacketed, configurations with different jacket lengths and locations are tested individually and the resulting resilience values as recorded are presented in Figure 4-6.

A 4-layer wrap of TU27C is used consistently for examining all the length configurations. It should be noted that for simplicity sake, identical partial jackets (with same length, thickness and location) are applied, on all the four bridge columns at a time, while examining each individual case. Hence, the resilience values are that of the bridge with all the columns wrapped identically using the indicated jacketing configuration. Each column is divided into six zones along its length that may or may not be jacketed. Figure 4-6 (a) shows the cases were partial jackets are provided symmetrically on column top and bottom in order to cover the most likely locations of plastic hinge formation. It can be gathered that jacketing just the ends and omitting the mid-length region has no impact on resilience whatsoever. This can be supported by the fact that the flexural rotational ductility values are consistently the highest in the middle third of the column. Figure 4-6 (b) shows the cases in which jacket length was varied uni-directionally starting from the top end. Likewise, the length was varied starting from the bottom end as shown in Figure 4-6 (c). It is observed that significant improvement in resilience occurs only for the case where the lower $5/6^{th}$ of the column or in other words, almost the entire length is jacketed. Based on the initial analysis, length of jacket was not defined as another variable in the optimization run. However, these results are factored by the specifics to the bridge model such as the column girder connection and possibly column slenderness ratios.

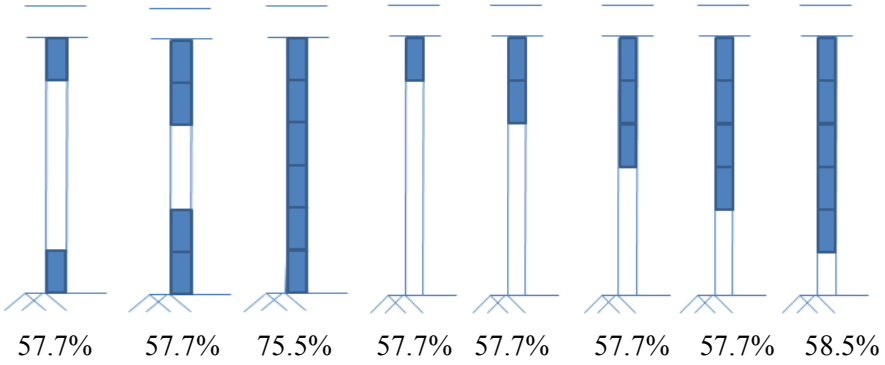

Figure 4-6 (a)

Figure 4-6 (b)

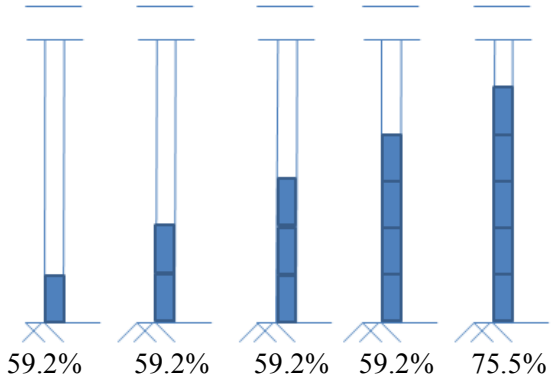

Figure 4-6 (c)

Figure 4-6. Partial jacketing length configurations (a) Symmetric jackets on column top and bottom, (b) Length varied from the top at column-girder connection, (c) Length varied from pier base.

Chapter 5

Summary and conclusions

This study presented optimization of column jacket retrofit design for an example Caltrans bridge by using the evolutionary computer algorithm Non-dominated Sorting Genetic Algorithm II. A two objective optimization analysis was conducted to maximize bridge seismic resilience while simultaneously minimizing cost investment in retrofit. The relative cost-benefits of three different retrofit materials prevalent in practice namely, A36 carbon steel, carbon/epoxy and glass/epoxy laminates were inspected by defining these as the available material options in the variable domain space. Additionally, the number of plies or thickness of jacket, and the choice of bridge columns to be retrofitted were defined as variable parameters in the search for optimal design configurations. The Matlab optimization program was run in conjunction with the OpenSees platform where, extensive non-linear time history analyses were performed to measure bridge response and thereby evaluate every design configuration generated by the search algorithm. In order to categorize bridge rotations into appropriate damage states, separate moment-curvature analyses were conducted initially to obtain the ultimate ductility values of every possible retrofitted section that may be generated.

The optimization analysis was conducted exhaustively by performing three separate runs to present optimal results for each material option. This was required; owing to the predominance of the carbon/epoxy solutions in the first run based on the rationale provided in section 4.3. The adopted population size and maximum number of generations seem reasonable based on the early convergence along with a fair distribution of solutions between the upper and lower bounds of achievable resilience. In addition, separate analysis was performed to investigate the effect of

partial jacketing on resilience and to identify the critical regions for confinement. The following conclusions may be made from the presented results:

1. All final generation optimal results point to the participation of only the interior columns in bridge flexural response to lateral loading.
2. For the particular case study the composite cost models are such that the glass/epoxy solutions do not have a clear advantage on the cost axis over the carbon/epoxy solutions, within the same range of resilience. Based on the Pareto fronts, the best compromise solution in the global run was identified as 3 layers of TU27C jacket around only the interior columns.
3. By examining the slope of the final Pareto front, a fair judgment on the best compromise solution within the glass/epoxy domain was made to be 2 plies of jacket on the interior columns only. The best exploitation on the resilience objective could be made at a 6 ply jacketing of the two interior columns again, and leaving the outer columns unretrofitted.
4. For the defined parameter domain for steel jacket, there was low sensitivity of resilience to increasing jacket thickness from 3/8 inch to 1 inch and therefore 3/8 inch jacketing of interior columns was identified as the singular optimal solution.
5. In varying the length of jacket or the region on the column to be jacketed, significant improvement in resilience occurs only for the case where the lower 5/6th of the column or in other words, almost the entire length was jacketed. It was gathered that length need not be defined as a variable in the optimization run for the particular case study bridge. It is recognized that these results are factored by the specifics to the bridge model such as the column girder connection and column slenderness ratio.

Further study

The optimization domain may be expanded to handle more complex multi-objective problems, by choosing an asymmetric bridge model and by incorporating into study other modes of failure and means of retrofit such as seismic isolation. In the modeling of composite column sections, the more recent and widely accepted Teng and Lam (2004) model may be adopted as opposed to the Mander model used in this study. Also, the cost model used in the retrofit cost evaluation may be modified to include installation and labor costs. The resilience study may be extended to an example bridge network using a well-defined indirect cost model that incorporates region-specific traffic information and network study.

References

Amdal, J. R., and Swigart, S. L. (2010). "Resilient transportation systems in a post-disaster environment: a case study of opportunities realized and missed in the greater New Orleans region." UNOTI Publications: Paper 5.

ACI. (2008). "Building Code Requirements for Structural Concrete (ACI 318-08) and Commentary." American Concrete Institute, Farmington Hills, MI.

API. (2000). "Recommended practice for planning, designing and constructing fixed offshore platforms." American Petroleum Institute (API), Recommended Practice 2A-WSD (RP 2A).

ATC-13. (1985). "Earthquake Damage Evaluation Data for California." Applied Technology Council, Redwood City, CA.

Arcidiacono, V., Cimellaro, G. P., Reinhorn, A. M., and Bruneau, M. (2012). "Community resilience evaluation including interdependencies." 15th World Conference on Earthquake Engineering (15WCEE), Lisbon, Portugal.

Banerjee, S. and Prasad, G. G. (2013). "Seismic Risk Assessment of Reinforced Concrete Bridges in Flood-Prone Regions." Structure and Infrastructure Engineering, 9(9), 952-968.

Banerjee, S. and Shinozuka, M. (2008a). "Mechanistic Quantification of RC Bridge Damage States under Earthquake through Fragility Analysis." Probabilistic Engineering Mechanics, 23(1), 12-22.

Banerjee, S. and Shinozuka, M. (2008b). "Experimental Verification of Bridge Seismic Damage States Quantified by Calibrating Analytical Models with Empirical Field Data." Journal of Earthquake Engineering and Engineering Vibration, 7(4), 383-393.

Boulanger, R.w., Curras, C.J., Kutter, B.L., Wilson, D.W., and Abghari, A. (1990). “Seismic Soil-pile-strcture interaction experiments and analysis." Journal of Geotechnical and Geoenvironmental Engineering, ASCS, 125(9):750-759.

Bruneau, M., Chang, S., Eguchi, R., Lee, G., O’Rourke, T., Reinhorn, A., Shinozuka, M., Tierney, K., Wallace, W., and von Winterfelt, D. (2003). “A framework to quantitatively assess and enhance the seismic resilience of communities.” Earthquake Spectra, 19 (4): 733-752.

Caltrans. (2008). “Bridge Standard Detail Sheets.” State of California Department of Transportation Division of Engineering Services. http://www.dot.ca.gov/hq/esc/techpubs/updates/page/bda-sec14-2.pdf

Casciati, F., Cimellaro, G. P., and Domaneschi, M. (2008). “Seismic reliability of a cable-stayed bridge retrofitted with hysteretic devices.” Computer and Structures 86, 1769-1781.

Chang, S., and Chamberlin, C. (2004). “Assessing the role of lifeline systems and community disaster resilience.” MCEER Research Progress and Accomplishments, Buffalo, NY.

Chang, S. E., and Nojima, N. (2001). “Measuring post-disaster transportation system performance: the 1995 Kobe earthquake in comparative perspective.” Transportation Research Part A: Policy and Practice, 35 (6): 475-494.

Cimellaro, G. P., Reinhorn, A. M., and Bruneau, M. (2010a). “Framework for analytical quantification of disaster resilience.” Engineering Structures ; 32: 3639-3649.

Cimellaro, G. P., Reinhorn, A. M., and Bruneau, M. (2010b). “Seismic resilience of a hospital system.” Structure and Infrastructure Engineering 6 (1-2), 127-144.

Cimellaro, G. P. (2013). “Resilience-based design (RBD) modelling of civil infrastructure to assess seismic hazards.” Handbook of Seismic Risk Analysis and Management of Civil

Infrastructure Systems, Edited by S. Tesfamariam, Canada and K. Goda, University of Bristol, UK, Woodhead Publishing Limited.

Cutter, S. L., Ahearn, J. A., Amadei, B., Crawford, P., Eide, E. A., Galloway, G. E., and Zoback, M. L. (2013). "Disaster Resilience: A National Imperative." Environment: Science and Policy for Sustainable Development, 55(2), 25-29.

Deb, K.. (2001). "Multi-objective Optimization using Evolutionary Algorithms," John Wiley & Sons, Ltd, West Sussex, England.

Deb, K., Pratap, A., Agarwal, S., and Meyarivan, T. (2002). "A Fast and Elitist Multiobjective Genetic Algorithm: NSGA-II," Evolutionary Computation, IEEE Transactions, 6(2), 182–197.

Decò, A., Bocchini, P., and Frangopol, D. M. (2013). "A probabilistic approach for the prediction of seismic resilience of bridges." Earthquake Engineering and Structural Dynamics, Available online DOI: 10.1002/eqe.2282.

Dennemann, L.K. (2009). "Life-Cycle Cost Benefit (LCC-B) Analysis for Bridge Seismic Retrofits." MS Thesis, Rice University, TX.

Ferrolho, A., & Crisóstomo, M. (2005). "Genetic Algorithms: concepts, techniques and applications." WSEAS Transactions on Advances in Engineering Education 2 (2005): 12.

Hajsadeghi, M., Alaee, F. J., and Shahmohammadi, A. (2011). "Investigation on behaviour of square/rectangular reinforced concrete columns retrofitted with FRP jacket." Journal of Civil Engineering and Management, 17(3), 400-408.

Haroun, M. and Elsanadedy, H. (2005). "Fiber-Reinforced Plastic Jackets for Ductility Enhancement of Reinforced Concrete Bridge Columns with Poor Lap-Splice Detailing." J. Bridge Eng., 10(6), 749–757.

HAZUS. (1999). “Earthquake Loss Estimation Methodology.” Technical Manual SR2, Federal Emergency Management Agency through agreements with National Institute of Building Science, Washington, D.C.

HAZUS–MH MR5. “Multi-hazard Loss Estimation Methodology – Earthquake Model.” Technical Manual, Department of Homeland Security, Washington, D.C.

Manyena, S. B. (2006). “The concept of resilience revisited.” Disasters, 30(4), 434-450.

McKenna, F., and G. L. Fenves. (2012). “Open System for Earthquake Engineering Simulation, Version 2.4.0.” Pacific Earthquake Engineering Research Center.

Paton, D., and Johnston, D. (2006). “Disaster Resilience an Integrated Approach.” Charles C Thomas Publisher LTD., Cap. 4, Lifelines and Urban Resilience. ISBN 0-398-07663-4 – ISBN 0-398-07664-2,

Pekcan, G. (1998). “Design of seismic energy dissipation systems for concrete and steel Structures.” Ph.D. Dissertation , State University of New York at Buffalo, New York.

Prasad, G. G. and Banerjee, S. (2013). “The Impact of Flood-Induced Scour on Seismic Fragility Characteristics of Bridges.” Journal of Earthquake Engineering, 17(9), 803-828.

Priestley, M.J.N., Seible, F., Calvi, G.M. (1996). “Seismic Design and Retrofit of Bridges.” John Wiley & Sons, Inc., New York, N.Y.

Priestley, M.J.N.; Seible, F.; Chai, Y.H. (1992). “Seismic retrofit of bridge columns using steel jackets.” Proceedings of the World Conference on Earthquake Engineering, p-5285.

Quakewrap Inc. “Product Data Sheets for Structural Strengthening”. http://www.quakewrap.com/product_data_sheets/TU27C.pdf, www.quakewrap.com/product_data_sheets/VU27G.pdf

Ramanathan, K., DesRoches, R., & Padgett, J. E. (2012). “A comparison of pre-and post-seismic design considerations in moderate seismic zones through the fragility assessment of multispan bridge classes.” Engineering Structures, 45, 559-573.

Rose, A., and Liao, S. E. (2005). "Modeling regional economic resiliency to earthquakes: a computable general equilibrium analysis of water service disruptions." Journal of Regional Science, 45: 75-112.

Saadatmanesh, H., Ehsani, M. R., and Li, M. W. (1994). "Strength and ductility of concrete columns externally reinforced with fiber composite straps." ACI Structural Journal, 91(4).

Seible, F. , Hegemier, G. A. , and Innamorato, D. (1995). "Developments in bridge column jacketing using advance composites." Proc., Nat. Seismic Conf. on Bridges and Hwy., Federal Highway Administration and California Department of Transportation, San Diego, Calif.

Shinozuka, M., Chang, S. E., Cheng, T. C., Feng, M., O'Rourke, T. D., Saadeghvaziri, M. A., Dong, X., Jin, X., Wang, Y., and Shi, P. (2004). "Resilience of integrated power and water systems." MCEER Research Progress and Accomplishments, 65-86. Buffalo, NY.

Sultan, M. and Kawashima, K. (1993). "Comparison of the seismic design of highway bridges in California and in Japan." Recent selected publications of Earthquake Engineering Div., Public Works Research Institute (PWRI), Japan (Technical Memorandum of PWRI No. 3276.

Teng, J. G., and Lam, L. (2004). "Behavior and modeling of fiber reinforced polymer-confined concrete." Journal of Structural Engineering, 130(11), 1713-1723.

Venkittaraman, A., and Banerjee, S. (2014). "Enhancing resilience of highway bridges through seismic retrofit." Earthquake Engineering & Structural Dynamics, 43(8), 1173-1191.

Wright, T., DesRoches, R., and Padgett, J.E. (2011). "Bridge Seismic Retrofitting Practices in the Central and Southeastern United States." Journal of Bridge Engineering, 16(1), 82-92.

WSDOT. (2011). “Washington State’s Bridge Seismic Retrofit Program”. http://www.wsdot.wa.gov/eesc/bridge/preservation/pdf%5CBrgSeismicPaper.pdf [February 14, 2011].

Zhou, Y., Banerjee, S., and Shinozuka, M. (2010). “Socio-economic effect of seismic retrofit of bridges for highway transportation networks: A pilot study.” Structure and Infrastructure Engineering, 6 (1–2), 145–157.